Article

Not peer-reviewed version

Histone Methyltransferase SsDim5 Regulates Fungal Virulence through H3K9 Trimethylation in Sclerotinia sclerotiorum

Lei Qin , Xin Gong , Jieying Nong , Xianyu Tang , Kan Cui , Yan Zhao , Shitou Xia *

Posted Date: 11 March 2024

doi: 10.20944/preprints202403.0552.v1

Keywords: S. sclerotiorum; Pathogenicity; Histone methylation; Mycotoxins; Stress.

Article

Histone Methyltransferase *Ss*Dim5 Regulates Fungal Virulence through H3K9 Trimethylation in *Sclerotinia sclerotiorum*

Lei Qin [1,†], Xin Gong [1,†], Jieying Nong [1], Xianyu Tang [1], Kan Cui [2], Yan Zhao [1] and Shitou Xia [1,*]

[1] Hunan Provincial Key Laboratory of Phytohormones and Growth Development, Hunan Agricultural University, Changsha 410128, China
[2] Institute of Plant Protection, Hunan Academy of Agricultural Sciences, Changsha 410125, China
* Correspondence: Shitou Xia (xstone0505@hunau.edu.cn)
† These authors contributed equally to this work.

Abstract: Histone post-translational modification is one of the main mechanisms of epigenetic regulation, which plays a crucial role in the control of gene expression and various biological processes. However, whether or not it affects fungal virulence is not clear in *Sclerotinia sclerotiorum*. In this study, we identified and cloned the histone methyltransferase *Defective in methylation 5* (*Dim5*) in *S. sclerotiorum*, which encodes a protein containing a typical SET domain. *SsDim5* was found to be dynamically expressed during infection. Knockout experiment demonstrated that deletion of *SsDim5* reduced the virulence in *Ssdim5-1*/*Ssdim5-2* mutant strains, accompanied by a significant decrease in H3K9 trimethylation levels. Transcriptomic analysis further revealed the downregulation of genes associated with mycotoxins biosynthesis in *SsDim5* deletion mutants. Additionally, the absence of *SsDim5* affected the fungus's response to oxidative and osmotic, as well as cellular integrity. Together, our results indicate that the H3K9 methyltransferase *Ss*Dim5 is essential for H3K9 trimethylation, which regulating fungal virulence to host plants through impacting on mycotoxins biosynthesis, and the response to environmental stresses in *S. sclerotiorum*.

Keywords: *S. sclerotiorum*; pathogenicity; histone methylation; mycotoxins; stress

1. Introduction

Sclerotinia sclerotiorum is a widespread fungal pathogen that parasitizes various hosts, causing severe diseases in over 600 plant species globally [1,2], which have significantly impact on the yield and quality of important economic crops such as canola and soybeans [3]. To successfully infect and parasitize its hosts, *S. sclerotiorum* has evolved complex and sophisticated infection strategies. In the early stages of infection, the fungus overcomes host defense responses through various pathways, establishing a short biotrophic phase, including the secretion of effectors and the formation of infection cushions [2]. Notably, *SsCmu1* is significantly upregulated during infection of *Brassica napus* [4], which encodes a secreted cutinase, capable of inhibiting host salicylic acid synthesis, thereby promoting infection [5]. Other putative effectors, such as *Ss*ITL [6], *Ss*CM1 [7], *Ss*CVNH [8], *Ss*v263 [9], and fungal effector proteins containing LysM domains, also exhibit high upregulation in the early infection stages, impacting the virulence of *S. sclerotiorum* [10]. After a brief biotrophic phase, the fungus induces host cell necrosis and cell wall degradation by producing numerous toxins, necrosis-inducing secreted proteins, and cell wall-degrading enzymes [2].

For pathogens, in order to adapt to changing host environments and defenses, infection processes require rapid and subtle adjustments to their gene expression programs. [11–13]. The regulation of gene expression is achieved at the transcriptional level through various mechanisms, include histone modification, as one of the primary epigenetic regulatory mechanisms, playing a particularly important role in shaping fungal pathogenicity [14]. Histones can undergo various covalent modifications, including methylation, acetylation, phosphorylation, and ubiquitination [15]. Histone methylation primarily occurs on the side chains of lysine and arginine. Lysine can undergo

 doi:10.20944/preprints202403.0552.v1

monomethylation, dimethylation, or trimethylation, while arginine may undergo monomethylation, symmetric dimethylation, or asymmetric demethylation [15,16]. Histone lysine methylation, a process orchestrated by histone lysine methyltransferases (HKMTs) with the SET domain, involves the transfer of a methyl group from S-adenosyl-L-methionine (SAM) to lysine residues at the N-terminus of H3 or H4 histones [17]. Typically, lysine 9 of histone H3 (H3K9) is linked to transcriptionally inactive heterochromatin, serving as a highly conserved epigenetic marker for heterochromatin formation and transcriptional silencing [18]. As a result, histone modifications play a crucial role in the regulation of gene expression, especially during the infection process. Through these modification mechanisms, fungi can flexibly respond to dynamic changes in the host environment.

H3K9 methylation is facilitated by specific proteins, including Clr4 (Cryptic loci regulator 4) in *Schizosaccharomyces pombe* and Dim5 (Defective in methylation 5) in *Neurospora crassa* [19]. In *Botrytis cinerea*, a plant pathogenic fungus, the absence of the *Dim5* gene results in a significant reduction of H3K9me3, causing the downregulation of pathogenic genes related to host signal perception, host tissue colonization, stress response, toxin synthesis, and host immune response [20]. In the maize pathogen *Fusarium verticillioides*, disruption of *Dim5* significantly reduces H3K9me3 levels, leading to a pronounced decrease in fungal virulence, accompanied by an unexpected increase in osmotic stress tolerance and expression of melanin synthesis genes [21]. In *Fusarium mangiferae*, the absence of the *KMT1* gene significantly impedes the biosynthesis of fumonisin and deoxynivalenol toxins in mango [22]. These indicate that the maintenance of H3K9me3 is crucial for the virulence of pathogenic fungi. However, currently there is no report on the biological function of H3K9me3 in *S. sclerotiorum.*

In this study, we characterized the histone H3 lysine methyltransferase *Ss*Dim5 by exploring its roles in H3 lysine trimethylation, regulation of mycotoxins synthesis, and pathogenicity as well as response to external stress, aimed to gain deeper insights into the physiological function of epigenetic regulation in the fungal pathogen *S. sclerotiorum*.

2. Materials and Methods

2.1. Fungal Strains, Plants, and Culture Conditions

The wild-type (WT) strain 1980 of *S. sclerotiorum* [23] was cultured on Potato Dextrose Agar (PDA), while the knockout mutants *Ssdim5-1*/*Ssdim5-2* were grown on PDA supplemented with 150 μg/mL hygromycin (Roche). The genetic complementation strain *SsDim5-C* was cultured on PDA containing 100 μg/mL Geneticin (G418). All these strains were incubated at 20°C.

Nicotiana benthamiana and *B. napus* (ZS11) plants used for pathogenicity tests were obtained from our laboratory stock and cultivated at 22°C with a 16-hour light/8-hour dark photoperiod.

2.2. Bioinformatics analysis of SsDim5

First, the genomic sequence of *BcDim5* from *B. cinerea* was obtained by accessing the NCBI database (http://www.ncbi.nlm.nih.gov/). BlastP analysis was then conducted to identify its orthologs in *S. sclerotiorum* and other species. Subsequently, multiple sequence alignment was performed using DNAMAN 6.0 (Lynnon BioSoft, Quebec, Canada). Finally, a phylogenetic tree was constructed using the Maximum Likelihood method with MEGA 6.0 software [24].

2.3. Gene knockout and genetic complementation of SsDim5

Refer to the previous method [25], sequences of the *SsDim5* gene were amplified using genomic DNA from WT strain 1980 as a template. Subsequently, these sequences were fused with the left and right portions of the hygromycin expression cassette, generating the gene knockout fragment. The knockout fragment was then introduced into WT protoplasts using PEG-mediated protoplast transformation [26]. Selection was performed by screening on PDA medium containing 150 mg/L hygromycin, resulting in the putative knockout transformants of *SsDim5*. Finally, through successive sub-culturing of mycelial tips, pure knockout strains were obtained and confirmed by PCR and qRT-PCR.

Simultaneously, using genomic DNA from the WT as a template, the sequence containing the full-length *SsDim5* gene, including its native promoter, was amplified. After digestion with *Kpn*I and

 doi:10.20944/preprints202403.0552.v1

*Eco*RI enzymes, this fragment was ligated into the linearized pCH-NEO1 vector. The vector containing the *SsDim5* gene fragment was introduced into the knockout mutant *Ssdim5-1* through Agrobacterium tumefaciens-mediated transformation, thereby obtaining a genetically complemented strain.

2.4. DNA extraction, RNA extraction and cDNA synthesis

Fresh mycelia were inoculated onto PDA plates covered with glass paper. Following a 2-day incubation, the mycelia were harvested, rapidly frozen in liquid nitrogen, and subsequently pulverized into powder. Genomic DNA extraction was performed using the cetyltrimethylammonium bromide (CTAB) method, as described by Allen et al. [27].

A commercial RNA extraction kit (AG21019, Accurate Biotechnology (Hunan) Co., Ltd., Changsha, China) was utilized for RNA extraction. Following the manufacturer's guidelines, first-strand cDNA synthesis was conducted using the Evo M-MLV reverse transcription kit (AG11705, Accurate Biotechnology (Hunan) Co., Ltd., Changsha, China).

2.5. Quantitative real-time PCR (qRT-PCR) analysis

The qRT-PCR experiments were conducted using the StepOne™ Real-Time PCR System and the SYBR® Green Premix Pro Taq HS qPCR Kit II (AG11702, Accurate Biotechnology (Hunan) Co., Ltd., Changsha, China). The PCR program consisted of 40 cycles, including an initial denaturation at 94°C for 2 minutes, denaturation at 94°C for 15 seconds, and annealing at 58°C for 1 minute. *SsTubulin1* was employed as the reference gene. The analysis of relative gene expression levels utilized the $2^{(-\Delta\Delta CT)}$ method [28].

2.6. Inoculation and virulence determination

Inoculation was performed following previously established protocols [29]. Mycelial plugs obtained from the actively growing colony edge were used for inoculating *N. benthamiana* and *B. napus* leaves (diameter 6 mm). Following inoculation, the leaves were cultured at 22°C with a relative humidity of 95-100%. Photographic documentation was carried out 24 hours post-infection.

2.7. Appressorium observation and oxalic acid analysis

Mycelial plugs (diameter 6 mm) were obtained from the actively growing edges. The mycelia were embedded in agar blocks and placed on glass slides. After 16 hours of incubation, the morphology and quantity of adherent cells were observed. Additionally, Mycelial plugs (diameter 1 mm) were inoculated onto the epidermis of onion epidermis. After 16 hours of invasion, the onion epidermis was stained in a 0.5% trypan blue solution for 30 minutes. Subsequently, bleaching solution (ethanol: acetic acid: glycerol = 3:1:1) was used for decolorization. Samples were observed and photographed using an optical microscope (Axio Imager 2, ZEISS, Oberkochen, Germany).

Furthermore, mycelial plugs (diameter 6 mm) were inoculated on PDA medium containing 100 μg/mL bromophenol blue to assess oxalic acid secretion.

2.8. Western blot analysis of H3K9 trimethylates

The mycelia were collected from PDA plates covered with glass paper membrane, approximately 500 mg in weight. After rapid freezing in liquid nitrogen and grinding, the mycelial powder was added to 100 μL of protein extraction buffer (200 mM pH = 6.8 Tris-HCl, 40% glycerol, 20% β-mercaptoethanol, 8% SDS, 0.4% bromophenol blue) for total protein extraction. The obtained proteins were then separated on a 10% denaturing polyacrylamide gel using sodium dodecyl sulfate-polyacrylamide gel electrophoresis (SDS-PAGE) and subsequently transferred to a nitrocellulose membrane using a Bio-Rad blotting apparatus.

After incubation with the primary antibody, incubation with the secondary antibody followed, and protein detection was carried out using the SuperSignal West Pico PLUS (product number: 34095, Thermo Scientific). The antibodies used, along with their sources and dilutions, were as follows: monoclonal antibody against histone H3 (Immunoway, 1:2000), monoclonal antibody against histone H3K9 (Abcam, 1:2000), and HRP-conjugated Rabbit anti-mouse IgG (1:5000).

 doi:10.20944/preprints202403.0552.v1

2.9. Abiotic stress response assay

To assess the response of the *Ssdim5-1*/*Ssdim-2* mutants to various stresses, we cultured them on PDA media supplemented with 1M NaCl, 1M KCl, 1M sorbitol, 0.005% SDS and 10mM H_2O_2, respectively. After incubation for 48 hours, we measured the mycelial diameter and calculated the growth inhibition rate using the formula: Growth Inhibition Rate (%) = 100 × (Colony diameter on pure PDA – Colony diameter under different stress conditions) / (Colony diameter on pure PDA).

2.10. RNA sequencing and data analysis

Cultures of WT and *Ssdim5-1* mutant mycelia, grown in PDB medium for 2 days, were harvested for transcriptome sequencing at Biomarker Technologies Corporation. Sequencing was performed on the Illumina NovaSeq platform according to the manufacturer's instructions, generating 150 bp paired-end sequences. During data cleaning, sequences containing adapters, poly-N sequences, and low-quality sequences were excluded to obtain high-quality clean data. Parameters such as Q20, Q30, GC content, and sequence duplication levels were computed. Following data validation, alignment to the reference genome sequence was executed. Gene functions were annotated through sequence alignment using various databases: Nr (NCBI non-redundant protein sequences), Pfam (protein families), KOG/COG (clusters of orthologous groups for eukaryotic complete genomes), Swiss-Prot (manually annotated and reviewed protein sequence database), KO (KEGG Ortholog database), and GO (gene ontology). Original counts were normalized using fragments per kilobase of transcript per million mapped reads (FPKM), and differential expression analysis was carried out with DESeq2. Genes meeting the criteria of a corrected p-value < 0.01 and a fold change ≥ 2, as determined by DESeq2 analysis, were considered differentially expressed. GO enrichment analysis of differentially expressed genes utilized the clusterProfiler package, employing the Wallenius non-central hypergeometric distribution.

3. Results

3.1. Identification of S. sclerotiorum histone H3K9 methyltransferase

In present, H3K9me3 modification is considered as an epigenetic mark that manipulates gene expression by regulating chromosomal accessibility [30]. To identify the H3K9 methyltransferase in the *S. sclerotiorum* and investigate its biological functions, we utilized the *B. cinerea Dim5* as a blast template and identified the homologous gene *SS1G_01550* in the *S. sclerotiorum* (hereafter referred to as *SsDim5*). Gene structure analysis revealed that *SsDim5* consists of three exons and two introns, encoding a peptide of 308 amino acid residues. Protein BLAST analysis indicated that Dim5 orthologs were widely distributed among species of the *Sclerotinia*, *Monilinia*, *Fusarium*, *Colletotrichum*, *Alternaria*, and *Rutstroemia P*. To analyze the phylogenetic relationships among Dim5 orthologs, we constructed a phylogenetic tree using Dim5 orthologs from the aforementioned species. The results indicated a close evolutionary relationship between *Ss*Dim5 and its ortholog in the *B. cinerea* (Figure 1A). Furthermore, protein structure analysis revealed that Dim5 orthologs from these species all contained the typical domains of H3K9 methyltransferase, including the PreSET domain, SET domain, and PostSET domain (Figure 1B). This suggests that these orthologs may possess histone modification activity, and the protein encoded by *SS1G_01550* in *S. sclerotiorum* is an ortholog of the *B. cinerea* Dim5.

 doi:10.20944/preprints202403.0552.v1

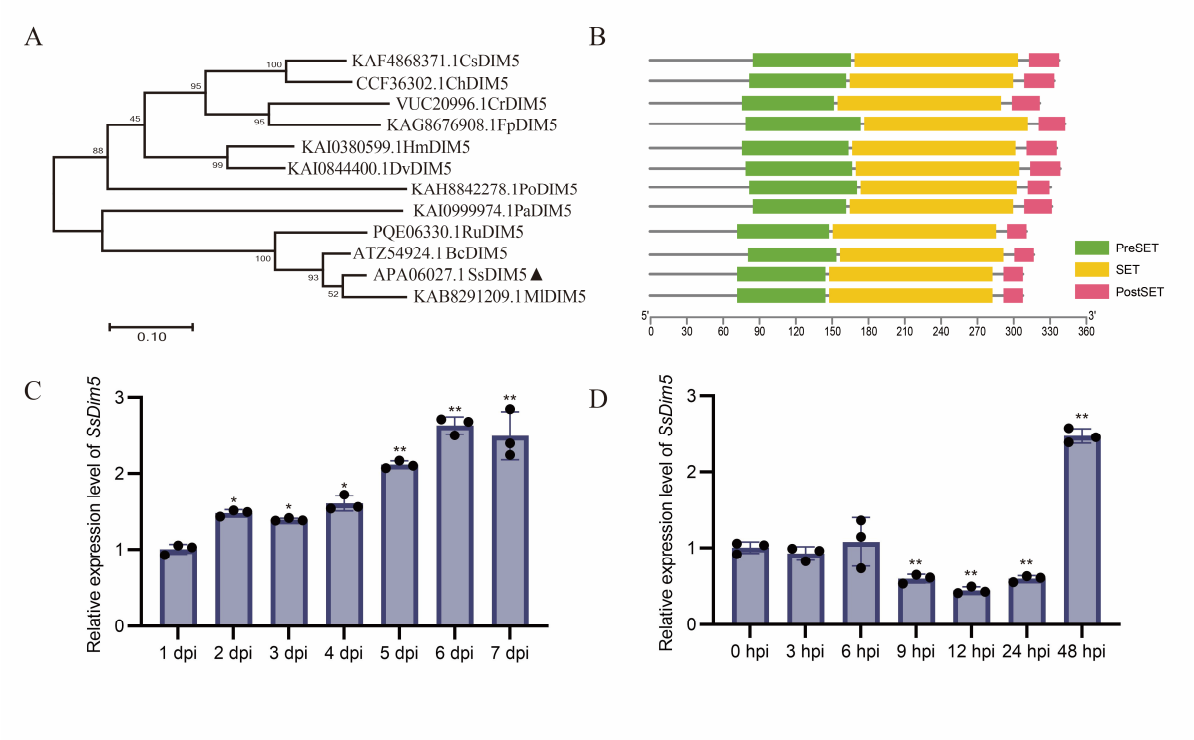

Figure 1. Phylogenetic tree, conserved protein domain and expression analysis of *SsDim5*. (**A**) Phylogenetic analysis of *Ss*Dim5 was conducted using the neighbour-joining method, aligning protein sequences with ClustalW based on JTT in MEGAX. Statistical confidence in the phylogenetic relationships was evaluated through 1000 bootstrap replicates. *Ss*Dim5 was marked with a black triangle, and UniProt database entry numbers were provided in brackets. (**B**) Conserved protein domains of *Ss*Dim5 and its orthologues were predicted using TBtool. (**C**) Expression levels of *SsDim5* at different growth stages of *S. sclerotiorum*. Utilizing *SsTubulin1* as the reference gene, average values and standard deviations were computed based on data from three independent biological replicates. Differences were evaluated using the one-way ANOVA test. * denotes $P<0.05$, ** denotes $P<0.01$. (**D**) Expression levels of *SsDim5* at different infection stages in *B. napus* leaves. Utilizing *SsTubulin1* as the reference gene, average values and standard deviations were computed based on data from three independent biological replicates. Differences were evaluated using the one-way ANOVA test. * denotes $P<0.05$, ** denotes $P<0.01$.

3.2. Expression patterns of SsDim5 during development and infection stages

In order to elucidate the regulatory functions of *SsDim5* during the developmental and invasive stages of the *S. sclerotiorum*, quantitative real-time PCR was employed to examine the accumulation of its transcripts at different stages. The expression profile revealed distinct expression patterns of *SsDim5* at various stages. Overall, during the developmental stage of the *S. sclerotiorum*, the expression of *SsDim5* showed an increasing trend, reaching its highest level during the formation and maturation stages of the sclerotia (Figure 1C). Conversely, during different stages of *S. sclerotiorum* infection on *B. napus* leaves, the expression of *SsDim5* was significantly suppressed initially at 9-24 hours post-infection, followed by a significant upregulation at 48 hours post-infection (Figure 1D). This indicates that *SsDim5* might play a crucial regulatory role in the formation of sclerotia and the infection process on the host.

3.3. Generation of SsDim5 knockout mutants and genetic complementation strains

To investigate the function of *SsDim5* within the *S. sclerotiorum*, a homologous recombination strategy was employed to generate two independent knockout mutants, *Ssdim5-1* and *Ssdim5-2* (Figure S1A). PCR analysis confirmed the absence of the *SsDim5* gene segment in both mutants, replaced by the HYG gene segment (Figure S1B). The results of qRT-PCR also indicated a lack of *SsDim5* transcript in the knockout mutants (Figure S1C). Subsequently, the accuracy of gene

 doi:10.20944/preprints202403.0552.v1

complementation in the *Ssdim5-1* mutant was validated by transforming the wild type *SsDim5* gene segment, including a 1500bp native-promoter, into the mutant strain. PCR and qRT-PCR further confirmed the accuracy of the gene complementation strain, designated as *SsDim5-C* (Figure S1B, C).

WT, two *SsDim5* knockout mutants (*Ssdim5-1*/*Ssdim5-2*), and the complementation strain *SsDim5-C* exhibited similar nutritional growth and developmental phenotypes on PDA medium. Further statistical analysis indicated no significant differences in growth rates among the strains (Figure 2A, B). Likewise, the number of sclerotium produced and the average weight of each sclerotium by *Ssdim5-1*/*Ssdim5-2* showed no significant differences compared to the WT and complementation strain on each culture plate (Figure 2C, D). These results imply that *Ss*Dim5 does not impact the mycelial growth and sclerotium formation of the *S. sclerotiorum*.

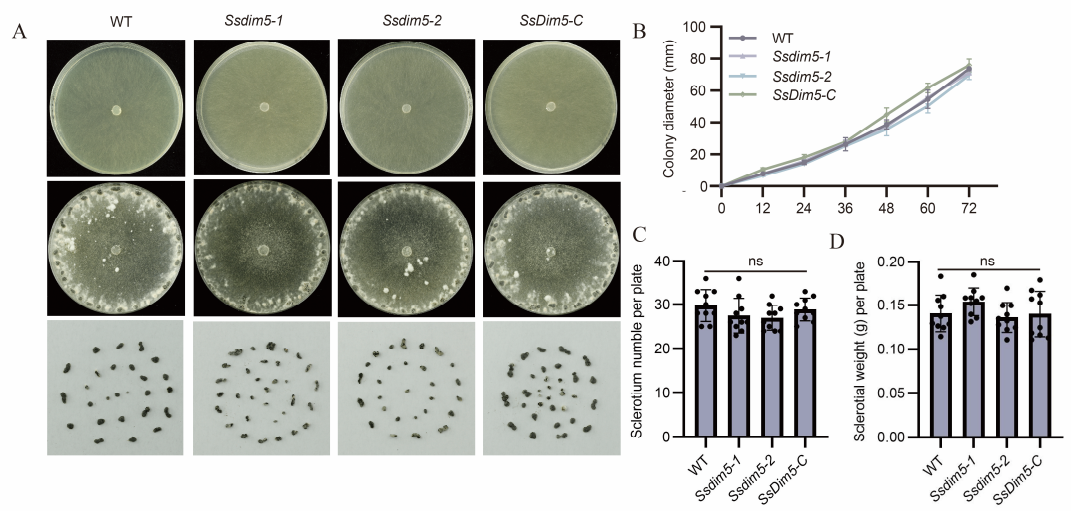

Figure 2. Phenotypes of *SsDim5* knockout and complemented strains. (**A**) Phenotypes of the WT, *SsDim5-1*, *SsDim5-2*, and *SsDim5-C*. One representative biological replicate was shown. (**B**) Radial growth length assessment on PDA of WT, *Ssdim5-1*, *Ssdim5-2*, and *SsDim5-C* strains. Average values and standard deviations were computed based on data from three independent biological replicates. (**C**) Number of sclerotia per plate. Average values and standard deviations were computed based on data from ten independent biological replicates. Differences were evaluated using the one-way ANOVA test. (**D**) Sclerotial weight per plate. Average values and standard deviations were computed based on data from ten independent biological replicates. Differences were evaluated using the one-way ANOVA test.

3.4. Deletion of SsDim5 impairs the virulence of S. sclerotiorum

To investigate the role of *SsDim5* in pathogenicity, isolated leaves of *B. napus* were inoculated with the WT strain, *SsDim5* knockout strains (*Ssdim5-1*/*Ssdim5-2*), and the complemented strain (*SsDim5-C*). After 24 hours of infection, the lesion areas caused by the knockout strains *Ssdim5-1*/*Ssdim5-2* were significantly smaller than that induced by the WT, whereas the lesion area caused by the complementation strain *SsDim5-C* resembled that of the WT (Figure 3A, B). Subsequently, each strain was employed to infect detached *N. benthamiana* leaves, and the infection outcomes mirrored those observed in *B. napus* leaves (Figure S2A, B). Notably, the virulence of the knockout strains *Ssdim5-1*/*Ssdim5-2* was significantly diminished both on *B. napus* and *N. benthamiana* leaves, suggesting that the reduced virulence is not specific to a particular host species.

 doi:10.20944/preprints202403.0552.v1

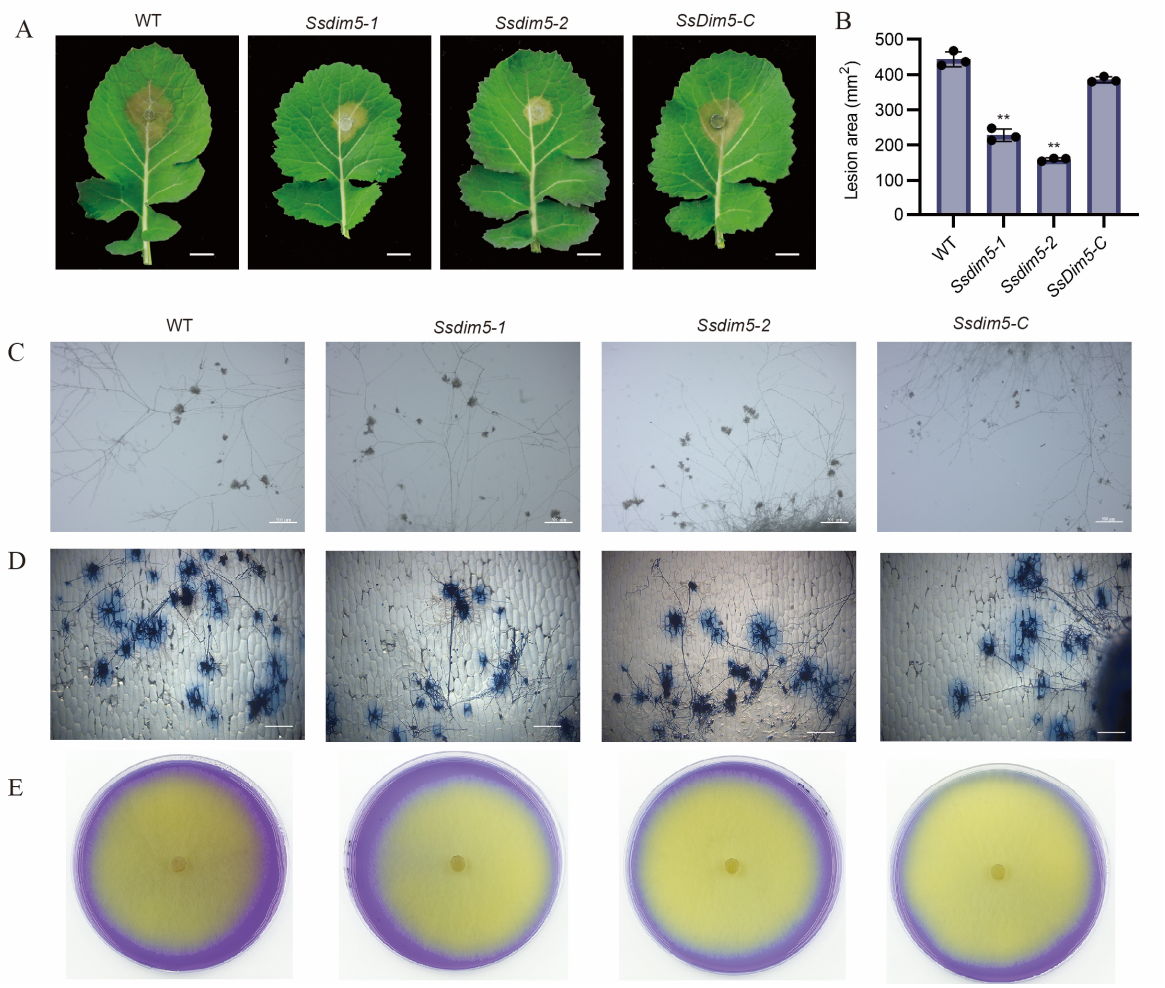

Figure 3. Pathogenicity assays of individual strains. (**A**) Disease phenotype of WT, *Ssdim5-1*, *Ssdim5-2* and *SsDim5-C* leaves of *B. napus*. Photographs were taken at 24 hpi. One representative biological replicate was shown. Bar = 1 cm. (**B**) Statistical analysis of the lesion area in panels. WT, *Ssdim5-1*, *Ssdim5-2* and *SsDim5-C*. Average values and standard deviations were computed based on data from three independent biological replicates. Differences were evaluated using the one-way ANOVA test. * denotes $P<0.05$, ** denotes $P<0.01$. Bar = 500 μm. (**C**) The morphology of the appressoria of each strain after 16 hours of inoculation on a glass slide under a stereomicroscope. (**D**) The morphology of the appressoria of each strain after 16 hours of inoculation on the onions epidermis under a stereomicroscope. Bar = 200 μm. (**E**) Mycelium of WT, *SsDim5-1*, *Ssdim5-2* and *Ssdim5-C* strains cultivated on PDA medium supplemented with bromophenol blue.

Appressorium formation and oxalic acid (OA) production are key strategies for regulating *S. sclerotiorum* virulence. Since the deletion of *SsDim5* exhibits a reduced virulence phenotype, the OA production and appressoria of the knockout strain *Ssdim5-1*/*Ssdim5-2* was tested. The results showed that the morphology and number of appressoria formed by the knockout strain *Ssdim5-1*/*Ssdim5-2* were similar to those of the WT and complemented strain (*SsDim5-C*), with no significant difference, whether on a glass slide (Figure 3C) or onion epidermal cells (Figure 3D). In addition, by detecting OA production on PDA supplemented with bromophenol blue, as shown in Figure 3E, the knockout strain *Ssdim5-1*/*Ssdim5-2* had the same phenotype as the WT and complemented strain *SsDim5-C*. These experiments indicate that *Ss*Dim5 plays a critical role in virulence, but not by affecting appressorium formation and OA production.

3.5. H3K9 trimethylation levels are significantly reduced in SsDim5 knockout mutants

To investigate the role of *SsDim5* in histone modification, Western blot analysis was employed to assess the levels of histone methylation in the WT strain, *Ssdim5-1*/*Ssdim5-2*, and *SsDim5-C*. When

 doi:10.20944/preprints202403.0552.v1

probed with an antibody against histone H3, all strains exhibited bands of similar size (Figure 4). However, noteworthy differences emerged when examining trimethylation at H3K9. Abundant specific bands corresponding to trimethylated H3K9 were detected in the WT strain and *SsDim5-C*, while the knockout strains *Ssdim5-1*/*Ssdim5-2* showed a complete absence of signals for trimethylated H3K9 (Figure 4), indicative of a crucial role of *Ss*Dim5 in H3K9 trimethylation.

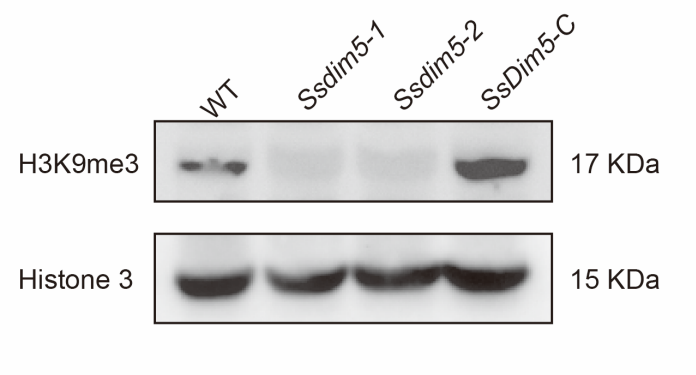

Figure 4. Western-blot analysis of *S. sclerotiorum* using antibodies histone H3 or trimethylated H3K9.

3.6. SsDim5 is related to the synthesis of mycotoxins

To further investigate the biological functions of *Ss*Dim5 in *S. sclerotiorum*, whole-genome expression profiling of the WT and *SsDim5* knockout strain (*Ssdim5-1*) mycelia was conducted through RNA sequencing (RNA-Seq). The results revealed 544 differentially expressed genes (DEGs), with 205 upregulated and 339 downregulated (p-value < 0.01 and fold change ≥2) (Figure 5A). Subsequently, an enrichment analysis based on Gene Ontology (GO) was performed on the DEGs, resulting in the assignment of 22 GO terms across three categories: biological processes (10 terms), cellular components (3 terms), and molecular functions (8 terms) (Figure S3). Notably, the biological process of "mycotoxins biosynthesis process" was significantly enriched in *Ssdim5-1* (Figure 5B). According to the transcriptional profile, among the 6 genes involved in "mycotoxins biosynthesis process", *SS1G_13355*, *SS1G_07229*, *SS1G_02251*, *SS1G_13850*, and *SS1G_13358* exhibited significantly lower expression levels in *Ssdim5-1* compared to the WT, while *SS1G_13636* showed significantly increased expression in *Ssdim5-1* (Figure 5C). qRT-PCR validation of these 6 genes in the WT, *Ssdim5-1*/*Ssdim5-2* and *SsDim5-C* further confirmed the consistent modulation pattern. Specifically, *SS1G_13355*, *SS1G_07229*, *SS1G_02251*, *SS1G_13850*, and *SS1G_13358* were suppressed in *Ssdim5-1* and *Ssdim5-2*, while *SS1G_13636* was enhanced in both *Ssdim5-1* and *Ssdim5-2* (Figure 5D). These findings suggest that *Ss*Dim5 regulates the synthesis of mycotoxins in *S. sclerotiorum*.

 doi:10.20944/preprints202403.0552.v1

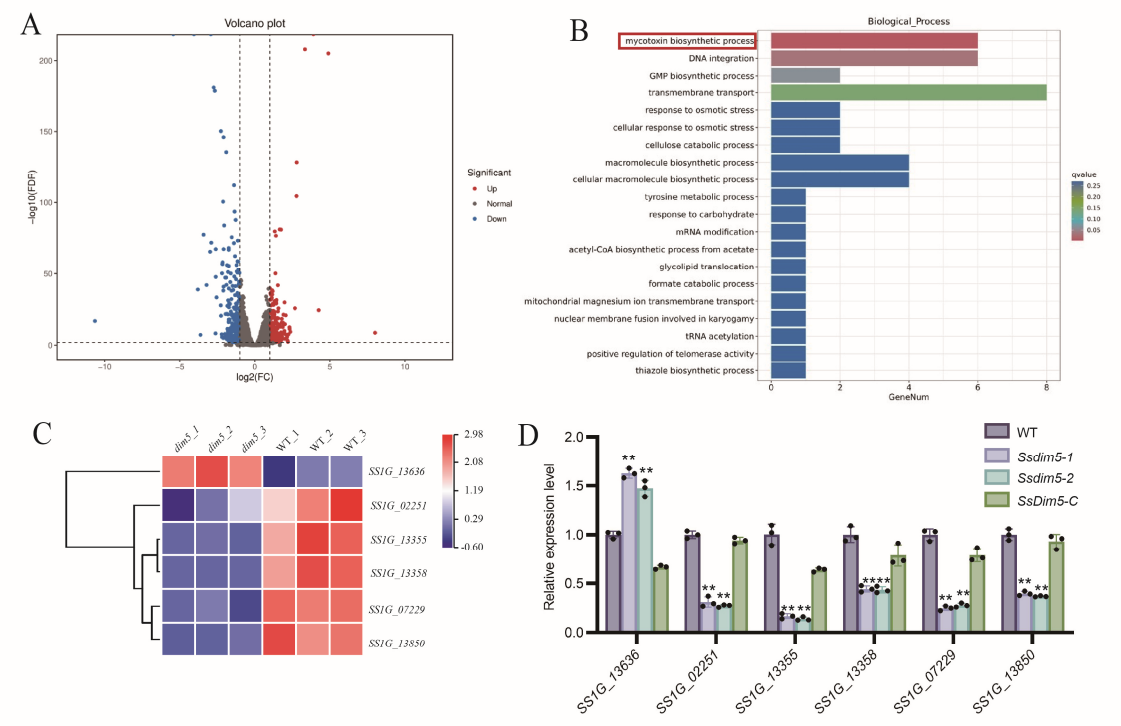

Figure 5. RNA-Seq analysis of WT and *Ss*Dim5 knockout strains. (**A**) The volcano plot of differentially expressed genes (DEGs) (*SsDim5* knockout strains vs. WT). (**B**) Significantly enriched Gene Ontology (GO) terms for all DEGs. (**C**) The expression profiles of mycotoxins biosynthesis genes. (**D**) The expression levels of mycotoxins biosynthesis genes by qRT-PCR. Utilizing *SsTubulin1* as the reference gene, average values and standard deviations were computed based on data from three independent biological replicates. Differences were evaluated using the one-way ANOVA test. * denotes $P<0.05$, ** denotes $P<0.01$.

3.7. Regulation of SsDim5 in Response to Environmental Stresses

The synthesis of mycotoxins is predominantly induced by factors such as oxidative stress, nutritional stress and various external environmental stimuli. To assess the role of *Ss*Dim5 in the resistance of *S. sclerotiorum* to external environmental stimuli, the growth performance of the WT, *Ssdim5-1*/*Ssdim5-2* knockout strains, and the complemented strain *SsDim5-C* was tested under different stress conditions. The growth inhibition rates of the *Ssdim5-1*/*Ssdim5-2* knockout strains were significantly higher than those of the WT strain and the complemented strain *SsDim5-C* on PDA plates containing 1M NaCl, 1M KCl, and 1M Sorbitol (Figure 6A, B). This indicates that *SsDim5* is associated with the high osmotic tolerance of *S. sclerotiorum*. Similarly, the growth inhibition rates of the *Ssdim5-1*/*Ssdim5-2* strains were higher than those of the WT and the complemented strain *SsDim5-C* on PDA plates containing 10mM H_2O_2 and 0.02% SDS, suggesting that *SsDim5* also plays a crucial regulatory role in oxidative stress and cell integrity in *S. sclerotiorum* (Figure 6A, B). Together, these results indicate that *SsDim5* plays a crucial regulatory role in the response of *S. sclerotiorum* to environmental stressors.

 doi:10.20944/preprints202403.0552.v1

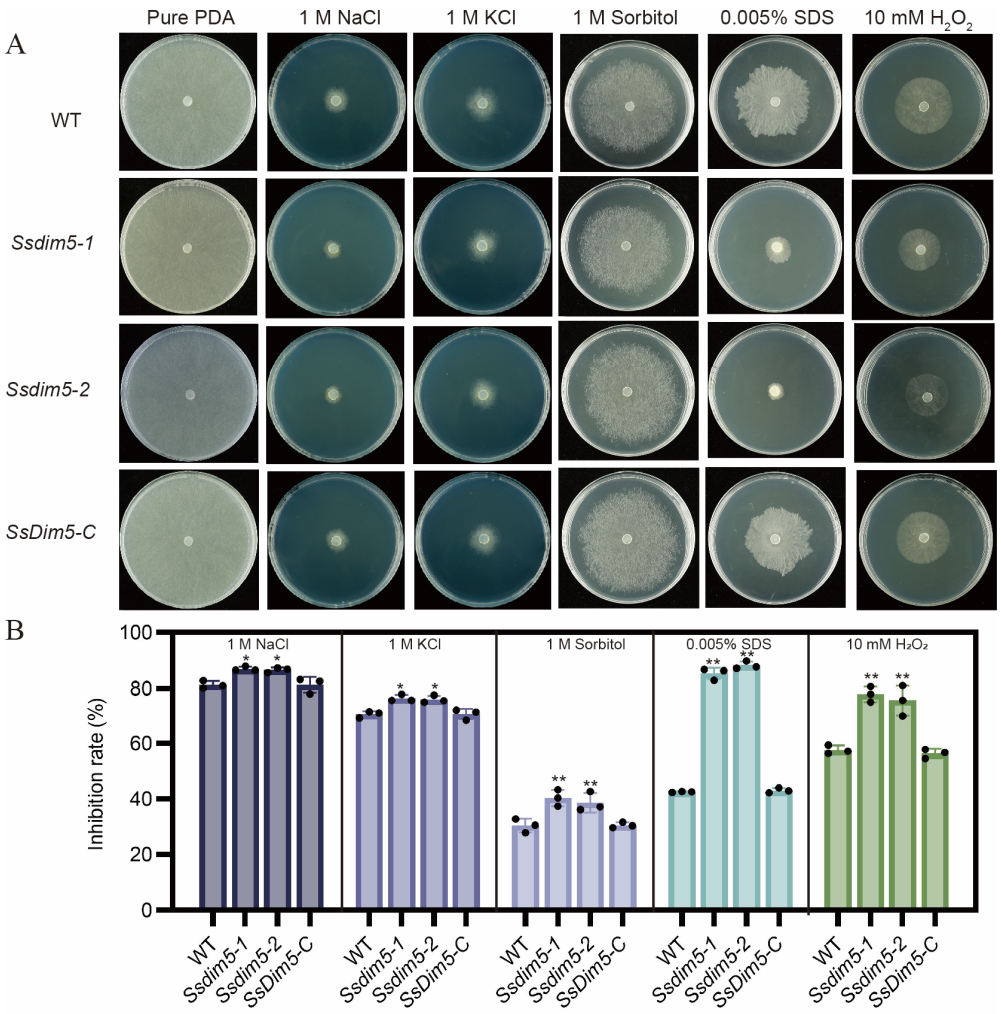

Figure 6. The growth of individual strains in the presence of various stressors. (**A**) Phenotypes of the WT, *Ssdim5-1*, *Ssdim5-2* and *SsDim5-C* supplemented with 1 M NaCl, 1 M KCl, 1 M Sorbitol, 0.005% SDS, 10 mM H_2O_2, respectively. (**B**) Statistics of inhibition rates under various stresses. Average values and standard deviations were computed based on data from three independent biological replicates. Differences were evaluated using the one-way ANOVA test. * denotes $P<0.05$, ** denotes $P<0.01$.

4. Discussion

In eukaryotes, lysine methylation modification of histones is mediated by histone lysine methyltransferases (KMT) [31], and H3K9 methylation relies on the activity of the KMT1 family [32]. Here, we identified a putative H3K9 methyltransferase, named *Ss*Dim5, by performing blast analysis on the protein sequence of the KMT1 family member *Bc*Dim5 in *B. cinerea*. *Ss*Dim5 is predicted to have a SET (Su(var)3–9, Enhancer-of-zeste, and Trithorax) domain, commonly associated with histone N-terminal lysine methyltransferase activity [33]. Previous studies have shown that human SUV39H1 and mouse Suv39h1 possess typical SET domains and catalyze directed H3K9 methylation modifications [34]. The Dim5 in *N. crassa* can specifically catalyze trimethylation of H3K9 [19]. In *S. pombe*, the histone methyltransferase Clr4 is responsible for monomethylation, dimethylation, and trimethylation of H3K9 [35]. Moreover, deletion of *BcDim5* in *B. cinerea* resulted in the loss of H3K9me3 [20]. Similar to previous results, western blot analysis indicates that H3K9me3 is nearly completely abolished in the *SsDim5* knockout mutant, and restored in the complemented strain, suggesting that *Ss*Dim5 indeed functions as an H3K9 methyltransferase *in vivo* and affects H3K9me3 in *S. sclerotiorum*. However, some studies have suggested that disruption of *Dim5* in *Beauveria bassiana* leads to the loss of H3K9me3 and a significant reduction in H3K4me1/me2, H3K9me1/me2, and

 doi:10.20944/preprints202403.0552.v1

H3K36me2 [36]. Therefore, it cannot be ruled out that *Ss*Dim5 in *S. sclerotiorum* may simultaneously possess other histone methylation modifications.

At different stages of growth, development, and infection, pathogens undergo extensive transcriptional reprogramming. H3K9 methylation is typically closely associated with heterochromatin formation, influencing various gene expressions by modulating chromosomal accessibility [30]. Through a gene knockout study of *Ss*Dim5 in *S. sclerotiorum*, we discovered an indispensable role for *Ss*Dim5 in the virulence of the fungus, without affecting its hyphal development and sclerotium formation. In the case of *N. crassa*, the absence of *TrDim5* resulted in impaired vegetative growth and conidiation [37]. The deletion mutant of *FvDim5* in *Fusarium graminearum* (*ΔFvDim5*) exhibited significant defects in conidiation, perithecium formation, and fungal virulence [21]. Similarly, the disruption of *BcDim5* in *B. cinerea* led to a significant reduction in hyphal growth, conidiophore production, and sclerotium yield, accompanied by a decrease in virulence [20]. Undoubtedly, our research results once again confirm the conservation of Dim5 in facilitating the physiological function of pathogen infection. However, there are also differences existed in Dim5 function among different species. In *S. sclerotiorum*, Dim5 is expressed at various stages of growth and development, yet no significant growth inhibition was observed through the observation of knockout mutants. Therefore, we speculate that *Ss*Dim5 may have redundant functions in the regulation of growth and development processes in *S. sclerotiorum*.

Genome sequencing has revealed that gene clusters involved in fungal secondary metabolism are often located near telomeres or heterochromatin regions [38]. H3K9 methylation, closely associated with the establishment of heterochromatin [39], has been demonstrated as an effective regulatory mechanism for disrupting or maintaining heterochromatin, impacting the generation of fungal secondary metabolites [40,41]. Here, RNA-seq analysis unveiled dysregulation in the expression of metabolism-related genes in the *SsDim5* knockout mutant, with significant enrichment observed in the pathway of mycotoxins biosynthesis through Gene Ontology (GO) analysis. Secondary metabolites (SM) play a crucial role in the virulence, development, and overall lifestyle of fungal pathogens. In the interaction between fungi and plant hosts, these metabolites may function as effectors while infecting the host and when recognized by the plant host during the infection process [42]. Mycotoxins biosynthesis is a subset of secondary metabolites often overproduced in response to external stressors. The main factors that enhance mycotoxin production include oxidative stress, nutritional stress, light stress, as well as environmental factors such as pH, temperature, water activity, fungicides, and plant secondary metabolites [43]. Studies have demonstrated that fungi regulate oxidative bursts through mycotoxins, enhancing ecological benefits [44]. qRT-PCR results confirmed a significant decrease in the expression of genes related to mycotoxins biosynthesis in *SsDim5* knockout mutant. Additionally, the *SsDim5* knockout strain exhibited increased sensitivity to osmotic stress, oxidative stress, and substances damaging cell integrity. Intriguingly, disturbances in the redox state of *S. sclerotiorum* affected the accumulation of OA [45], impacting the levels of osmotic stress, high salt, and cell wall stress-related functional genes that influence virulence [46–50]. Therefore, it can be inferred that in *S. sclerotiorum*, the normal function of Dim5 is crucial for the synthesis of fungal secondary metabolites, especially mycotoxins, directly or indirectly influencing the virulence of *S. sclerotiorum* to host plants.

5. Conclusions

In summary, our results indicate that *Ss*Dim5 possesses histone H3 lysine methyltransferase activity, and plays a crucial regulatory role in the pathogenicity of *S. sclerotiorum* through the regulation of fungal mycotoxins biosynthesis, and the response to external stressors, thereby provides theoretical guidance for the development of new target points for the prevention and control of Sclerotinia stem rot.

Supplementary Materials: The following supporting information can be downloaded at the website of this paper posted on Preprints.org, **Figure S1.** Identification of *SsDim5* knockout mutants and genetically complemented strains. **Figure S2.** Pathogenicity assays of individual strains in *N. benthamiana* leaves. **Figure S3.** GO enrichment analysis of differentially expressed genes in *SsDim5* mutants. **T**able S1: Primers used in the experiment.

Author Contributions: L.Q. X.G. and S.X. planned and designed the research. L.Q., X.G., J.N., X.T., and Y.Z. performed research. L.Q., X.G., and X.T. conducted bioinformatics analysis. L.Q. and X.G. analyzed and validated the data. L.Q., J.N., and K.C. conducted transcriptome analysis. L.Q., X.G., and S.X. wrote the original draft of the manuscript. All authors discussed the data, edited, and approved the manuscript.

Funding: This research was funded by National Natural Science Foundation of China (grant 31971836).

Institutional Review Board Statement: Not applicable.

Informed Consent Statement: Not applicable.

Data Availability Statement: The data presented in this study are available on request from the corresponding author.

Acknowledgments: We cordially thank Dr. Daohong Jiang (Huazhong Agricultural University) for sharing pCH-EF-1 plasmid, and Jeffrey Rollins (University of Florida) for sharing WT *S. sclerotiorum* strain 1980.

Conflicts of Interest: The authors declare no conflict of interest.

References

1. Boland, G.J.; Hall, R. Index of plant hosts of *Sclerotinia sclerotiorum*. *Canadian Journal of Plant Pathology* **1994**, *16*, 93-108.
2. Liang, X.; Rollins, J.A. Mechanisms of Broad Host Range Necrotrophic Pathogenesis in *Sclerotinia sclerotiorum*. *Phytopathology* **2018**, *108*, 1128-1140, doi:10.1094/phyto-06-18-0197-rvw.
3. Bolton, M.D.; Thomma, B.P.H.J.; Nelson, B.D. *Sclerotinia sclerotiorum* (Lib.) de Bary: Biology and molecular traits of a cosmopolitanPathogen. *Molecular Plant Pathology* **2010**, *7*, 1-16.
4. Burketová, M.N.a.I.D.V. Plant hormones in defense response of *Brassica napus* to *Sclerotinia sclerotiorum* - Reassessing the role of salicylic acid in the interaction with a necrotroph. *Plant Physiology and Biochemistry* **2014**, *80*.
5. Djamei, A.; Schipper, K.; Rabe, F.; Ghosh, A.; Vincon, V.; Kahnt, J.; Osorio, S.; Tohge, T.; Fernie, A.R.; Feussner, I.; et al. Metabolic priming by a secreted fungal effector. *Nature* **2011**, *478*, 395-398, doi:10.1038/nature10454.
6. Zhu, W.; Wei, W.; Fu, Y.; Cheng, J.; Xie, J.; Li, G.; Yi, X.; Kang, Z.; Dickman, M.B.; Jiang, D. A secretory protein of necrotrophic fungus *Sclerotinia sclerotiorum* that suppresses host resistance. *PLoS One* **2013**, *8*, e53901, doi:10.1371/journal.pone.0053901.
7. Kabbage, M.; Williams, B.; Dickman, M.B. Cell death control: the interplay of apoptosis and autophagy in the pathogenicity of *Sclerotinia sclerotiorum*. *PLoS Pathog* **2013**, *9*, e1003287, doi:10.1371/journal.ppat.1003287.
8. Lyu, X.; Shen, C.; Fu, Y.; Xie, J.; Jiang, D.; Li, G.; Cheng, J. Comparative genomic and transcriptional analyses of the carbohydrate-active enzymes and secretomes of phytopathogenic fungi reveal their significant roles during infection and development. *Sci Rep* **2015**, *5*, 15565, doi:10.1038/srep15565.
9. Liang, Y.; Yajima, W.; Davis, M.R.; Kav, N.N.V.; Strelkov, S.E. Disruption of a gene encoding a hypothetical secreted protein from *Sclerotinia sclerotiorum* reduces its virulence on canola (*Brassica napus*). *Canadian Journal of Plant Pathology* **2013**, *35*, 46-55.
10. Sánchez-Vallet, A.; Tian, H.; Rodriguez-Moreno, L.; Valkenburg, D.J.; Saleem-Batcha, R.; Wawra, S.; Kombrink, A.; Verhage, L.; de Jonge, R.; van Esse, H.P.; et al. A secreted LysM effector protects fungal hyphae through chitin-dependent homodimer polymerization. *PLoS Pathog* **2020**, *16*, e1008652, doi:10.1371/journal.ppat.1008652.
11. Gómez-Díaz, E.; Jordà, M.; Peinado, M.A.; Rivero, A. Epigenetics of host-pathogen interactions: the road ahead and the road behind. *PLoS Pathog* **2012**, *8*, e1003007, doi:10.1371/journal.ppat.1003007.
12. Zhu, Q.H.; Shan, W.X.; Ayliffe, M.A.; Wang, M.B. Epigenetic Mechanisms: An Emerging Player in Plant-Microbe Interactions. *Mol Plant Microbe Interact* **2016**, *29*, 187-196, doi:10.1094/mpmi-08-15-0194-fi.
13. Lai, Y.; Chen, H.; Wei, G.; Wang, G.; Li, F.; Wang, S. In vivo gene expression profiling of the entomopathogenic fungus *Beauveria bassiana* elucidates its infection stratagems in Anopheles mosquito. *Sci China Life Sci* **2017**, *60*, 839-851, doi:10.1007/s11427-017-9101-3.
14. Meile, L.; Peter, J.; Puccetti, G.; Alassimone, J.; McDonald, B.A.; Sánchez-Vallet, A. Chromatin Dynamics Contribute to the Spatiotemporal Expression Pattern of Virulence Genes in a Fungal Plant Pathogen. *mBio* **2020**, *11*, doi:10.1128/mBio.02343-20.
15. Lan, F.; Shi, Y. Epigenetic regulation: methylation of histone and non-histone proteins. *Sci China C Life Sci* **2009**, *52*, 311-322, doi:10.1007/s11427-009-0054-z.
16. Bedford, M.T.; Clarke, S.G. Protein arginine methylation in mammals: who, what, and why. *Mol Cell* **2009**, *33*, 1-13, doi:10.1016/j.molcel.2008.12.013.
17. Brosch, G.; Loidl, P.; Graessle, S. Histone modifications and chromatin dynamics: a focus on filamentous fungi. *FEMS Microbiol Rev* **2008**, *32*, 409-439, doi:10.1111/j.1574-6976.2007.00100.x.

18. Berger, S.L. The complex language of chromatin regulation during transcription. *Nature* **2007**, *447*, 407-412, doi:10.1038/nature05915.
19. Freitag, M. Histone Methylation by SET Domain Proteins in Fungi. *Annu Rev Microbiol* **2017**, *71*, 413-439, doi:10.1146/annurev-micro-102215-095757.
20. Zhang, X.; Liu, X.; Zhao, Y.; Cheng, J.; Xie, J.; Fu, Y.; Jiang, D.; Chen, T. Histone H3 Lysine 9 Methyltransferase DIM5 Is Required for the Development and Virulence of *Botrytis cinerea*. *Front Microbiol* **2016**, *7*, 1289, doi:10.3389/fmicb.2016.01289.
21. Gu, Q.; Ji, T.; Sun, X.; Huang, H.; Zhang, H.; Lu, X.; Wu, L.; Huo, R.; Wu, H.; Gao, X. Histone H3 lysine 9 methyltransferase FvDim5 regulates fungal development, pathogenicity and osmotic stress responses in *Fusarium verticillioides*. *FEMS Microbiol Lett* **2017**, *364*, doi:10.1093/femsle/fnx184.
22. Atanasoff-Kardjalieff, A.K.; Lünne, F.; Kalinina, S.; Strauss, J.; Humpf, H.U.; Studt, L. Biosynthesis of Fusapyrone Depends on the H3K9 Methyltransferase, FmKmt1, in *Fusarium mangiferae*. *Front Fungal Biol* **2021**, *2*, 671796, doi:10.3389/ffunb.2021.671796.
23. Godoy, G.; Steadman, J.R.; Dickman, M.B.; Dam, R. Use of mutants to demonstrate the role of oxalic acid in pathogenicity of *Sclerotinia sclerotiorum* on Phaseolus vulgaris. *Physiological & Molecular Plant Pathology* **1990**, *37*, 179-191.
24. Chenna, R.; Sugawara, H.; Koike, T.; Lopez, R.; Gibson, T.J.; Higgins, D.G.; Thompson, J.D. Multiple sequence alignment with the Clustal series of programs. *Nucleic Acids Res* **2003**, *31*, 3497-3500, doi:10.1093/nar/gkg500.
25. Qin, L.; Nong, J.; Cui, K.; Tang, X.; Gong, X.; Xia, Y.; Xu, Y.; Qiu, Y.; Li, X.; Xia, S. SsCak1 Regulates Growth and Pathogenicity in *Sclerotinia sclerotiorum*. *Int J Mol Sci* **2023**, *24*, doi:10.3390/ijms241612610.
26. Lan, C.; Qiao, L.; Niu, D. *Sclerotinia sclerotiorum* Protoplast Preparation and Transformation. *Bio Protoc* **2023**, *13*, e4581, doi:10.21769/BioProtoc.4581.
27. Allen, G.C.; Flores-Vergara, M.A.; Krasynanski, S.; Kumar, S.; Thompson, W.F. A modified protocol for rapid DNA isolation from plant tissues using cetyltrimethylammonium bromide. *Nat Protoc* **2006**, *1*, 2320-2325, doi:10.1038/nprot.2006.384.
28. Livak, K.J.; Schmittgen, T.D. Analysis of relative gene expression data using real-time quantitative PCR and the 2(-Delta Delta C(T)) Method. *Methods* **2001**, *25*, 402-408, doi:10.1006/meth.2001.1262.
29. Mei, J.; Liu, Y.; Wei, D.; Wittkop, B.; Ding, Y.; Li, Q.; Li, J.; Wan, H.; Li, Z.; Ge, X.; et al. Transfer of sclerotinia resistance from wild relative of Brassica oleracea into *Brassica napus* using a hexaploidy step. *Theor Appl Genet* **2015**, *128*, 639-644, doi:10.1007/s00122-015-2459-3.
30. Gessaman, J.D.; Selker, E.U. Induction of H3K9me3 and DNA methylation by tethered heterochromatin factors in *Neurospora crassa*. *Proc Natl Acad Sci U S A* **2017**, *114*, E9598-e9607, doi:10.1073/pnas.1715049114.
31. Kouzarides, T. Chromatin modifications and their function. *Cell* **2007**, *128*, 693-705, doi:10.1016/j.cell.2007.02.005.
32. Allis, C.D.; Berger, S.L.; Cote, J.; Dent, S.; Jenuwien, T.; Kouzarides, T.; Pillus, L.; Reinberg, D.; Shi, Y.; Shiekhattar, R.; et al. New nomenclature for chromatin-modifying enzymes. *Cell* **2007**, *131*, 633-636, doi:10.1016/j.cell.2007.10.039.
33. Eissenberg, J.C.; James, T.C.; Foster-Hartnett, D.M.; Hartnett, T.; Ngan, V.; Elgin, S.C. Mutation in a heterochromatin-specific chromosomal protein is associated with suppression of position-effect variegation in Drosophila melanogaster. *Proc Natl Acad Sci U S A* **1990**, *87*, 9923-9927, doi:10.1073/pnas.87.24.9923.
34. Rea, S.; Eisenhaber, F.; O'Carroll, D.; Strahl, B.D.; Sun, Z.W.; Schmid, M.; Opravil, S.; Mechtler, K.; Ponting, C.P.; Allis, C.D.; et al. Regulation of chromatin structure by site-specific histone H3 methyltransferases. *Nature* **2000**, *406*, 593-599, doi:10.1038/35020506.
35. Kusevic, D.; Kudithipudi, S.; Iglesias, N.; Moazed, D.; Jeltsch, A. Clr4 specificity and catalytic activity beyond H3K9 methylation. *Biochimie* **2017**, *135*, 83-88, doi:10.1016/j.biochi.2017.01.013.
36. Ren, K.; Mou, Y.N.; Tong, S.M.; Ying, S.H.; Feng, M.G. DIM5/KMT1 controls fungal insect pathogenicity and genome stability by methylation of histone H3K4, H3K9 and H3K36. *Virulence* **2021**, *12*, 1306-1322, doi:10.1080/21505594.2021.1923232.
37. Wang, L.; Liu, J.; Li, X.; Lyu, X.; Liu, Z.; Zhao, H.; Jiao, X.; Zhang, W.; Xie, J.; Liu, W. A histone H3K9 methyltransferase Dim5 mediates repression of sorbicillinoid biosynthesis in *Trichoderma reesei*. *Microb Biotechnol* **2022**, *15*, 2533-2546, doi:10.1111/1751-7915.14103.
38. Nierman, W.C.; Pain, A.; Anderson, M.J.; Wortman, J.R.; Kim, H.S.; Arroyo, J.; Berriman, M.; Abe, K.; Archer, D.B.; Bermejo, C.; et al. Genomic sequence of the pathogenic and allergenic filamentous fungus *Aspergillus fumigatus*. *Nature* **2005**, *438*, 1151-1156, doi:10.1038/nature04332.
39. Audergon, P.N.; Catania, S.; Kagansky, A.; Tong, P.; Shukla, M.; Pidoux, A.L.; Allshire, R.C. Epigenetics. Restricted epigenetic inheritance of H3K9 methylation. *Science* **2015**, *348*, 132-135, doi:10.1126/science.1260638.

40. Reyes-Dominguez, Y.; Bok, J.W.; Berger, H.; Shwab, E.K.; Basheer, A.; Gallmetzer, A.; Scazzocchio, C.; Keller, N.; Strauss, J. Heterochromatic marks are associated with the repression of secondary metabolism clusters in *Aspergillus nidulans*. *Mol Microbiol* **2010**, *76*, 1376-1386, doi:10.1111/j.1365-2958.2010.07051.x.
41. Reyes-Dominguez, Y.; Boedi, S.; Sulyok, M.; Wiesenberger, G.; Stoppacher, N.; Krska, R.; Strauss, J. Heterochromatin influences the secondary metabolite profile in the plant pathogen *Fusarium graminearum*. *Fungal Genet Biol* **2012**, *49*, 39-47, doi:10.1016/j.fgb.2011.11.002.
42. Stępień, Ł.; Lalak-Kańczugowska, J.; Witaszak, N.; Urbaniak, M. Fusarium Secondary Metabolism Biosynthetic Pathways: So Close but So Far Away. **2019**.
43. Reverberi, M.; Ricelli, A.; Zjalic, S.; Fabbri, A.A.; Fanelli, C. Natural functions of mycotoxins and control of their biosynthesis in fungi. *Appl Microbiol Biotechnol* **2010**, *87*, 899-911, doi:10.1007/s00253-010-2657-5.
44. Reverberi, M.; Fabbri, A.A.; Zjalic, S.; Ricelli, A.; Punelli, F.; Fanelli, C. Antioxidant enzymes stimulation in *Aspergillus parasiticus* by Lentinula edodes inhibits aflatoxin production. *Appl Microbiol Biotechnol* **2005**, *69*, 207-215, doi:10.1007/s00253-005-1979-1.
45. Kim, H.J.; Chen, C.; Kabbage, M.; Dickman, M.B. Identification and characterization of *Sclerotinia sclerotiorum* NADPH oxidases. *Appl Environ Microbiol* **2011**, *77*, 7721-7729, doi:10.1128/aem.05472-11.
46. Fan, H.; Yu, G.; Liu, Y.; Zhang, X.; Liu, J.; Zhang, Y.; Rollins, J.A.; Sun, F.; Pan, H. An atypical forkhead-containing transcription factor SsFKH1 is involved in sclerotial formation and is essential for pathogenicity in *Sclerotinia sclerotiorum*. *Mol Plant Pathol* **2017**, *18*, 963-975, doi:10.1111/mpp.12453.
47. Lyu, X.; Shen, C.; Fu, Y.; Xie, J.; Jiang, D.; Li, G.; Cheng, J. The Microbial Opsin Homolog Sop1 is involved in *Sclerotinia sclerotiorum* Development and Environmental Stress Response. *Frontiers in Microbiology* **2016**, *6*, 1504.
48. Veluchamy, S.; Williams, B.; Kim, K.; Dickman, M.B. The CuZn superoxide dismutase from *Sclerotinia sclerotiorum* is involved with oxidative stress tolerance, virulence, and oxalate production. *Physiological and Molecular Plant Pathology* **2012**, *78*, 14-23.
49. Xu, L.; Chen, W. Random T-DNA mutagenesis identifies a Cu/Zn superoxide dismutase gene as a virulence factor of *Sclerotinia sclerotiorum*. *Mol Plant Microbe Interact* **2013**, *26*, 431-441, doi:10.1094/mpmi-07-12-0177-r.
50. Yu, Y.; Xiao, J.; Yang, Y.; Bi, C.; Qing, L.; Tan, W. Ss-Bi1 encodes a putative BAX inhibitor-1 protein that is required for full virulence of *Sclerotinia sclerotiorum*. *Physiological & Molecular Plant Pathology* **2015**, *90*, 115-122.